

Evaluation of Ground Motion Scaling Methods for Analysis of Structural Systems

A.P. O'Donnell,¹ O.A. Beltsar,² Y.C. Kurama,³ E. Kalkan,⁴ A.A. Taflanidis⁵

¹Civil Engineering and Geological Sciences, Univ. of Notre Dame, 156 Fitzpatrick Hall, Notre Dame, IN 46556; PH: (617) 797-2311; email: aodonnell@nd.edu

²Civil Engineering and Geological Sciences, Univ. of Notre Dame, 156 Fitzpatrick Hall, Notre Dame, IN 46556; PH: (925) 353-0355; email: obeltsar@nd.edu

³Civil Engineering and Geological Sciences, Univ. of Notre Dame, 156 Fitzpatrick Hall, Notre Dame, IN 46556; PH: (574) 631-8377; email: ykurama@nd.edu

⁴Earthquake Science Center, United States Geological Survey, 345 Middlefield Rd., Menlo Park, CA 94025; PH: (650) 329-5146; email: ekalkan@usgs.gov

⁵Civil Engineering and Geological Sciences, Univ. of Notre Dame, 156 Fitzpatrick Hall, Notre Dame, IN 46556; PH: (574) 631-5696; email: a.taflanidis@nd.edu

ABSTRACT

Ground motion selection and scaling comprises undoubtedly the most important component of any seismic risk assessment study that involves time-history analysis. Ironically, this is also the single parameter with the least guidance provided in current building codes, resulting in the use of mostly subjective choices in design. The relevant research to date has been primarily on single-degree-of-freedom systems, with only a few studies using multi-degree-of-freedom systems. Furthermore, the previous research is based solely on numerical simulations with no experimental data available for the validation of the results. By contrast, the research effort described in this paper focuses on an experimental evaluation of selected ground motion scaling methods based on small-scale shake-table experiments of re-configurable linear-elastic and nonlinear multi-story building frame structure models. Ultimately, the experimental results will lead to the development of guidelines and procedures to achieve reliable demand estimates from nonlinear response history analysis in seismic design. In this paper, an overview of this research effort is discussed and preliminary results based on linear-elastic dynamic response are presented.

INTRODUCTION

As performance-based considerations become pre-requisite in the seismic design and evaluation of building structures, the use of nonlinear response history analysis (RHA) has gained utmost importance (e.g., for tall or irregular structures, structures with innovative structural systems and materials, and/or structures on soft soil). This rigorous analysis method requires, as input, a suite of ground motion records that have been selected and modified (i.e., scaled) appropriately to make them compatible with the site-specific hazard level(s) considered [e.g., Maximum Considered Earthquake (MCE) level, Design Basis Earthquake (DBE) level]. Ground motion selection and scaling has a large impact on the nonlinear RHA results. In fact, the ground motion record itself is undeniably the most important variable for nonlinear RHA (more than the analytical model parameters) governing the outcome and amount of uncertainty from seismic design.

Ironically, this is also the single parameter with the least guidance provided in current building codes and provisions, resulting in the use of mostly subjective choices in the selection of ground motions for nonlinear RHA.

Most of the research to date on ground motion scaling has been on single-degree-of-freedom systems (Chopra and Chinatanapakdee 2004; Martinez-Rueda 1998) with only a few studies on multi-degree-of-freedom systems (Kalkan and Chopra 2010, 2011; Kalkan and Kwong 2011; Alavi and Krawinkler 2000; Kurama and Farrow 2003; Shome and Cornell 1998). Furthermore, the previous research is based solely on numerical simulations, with no experimental data available for the validation of the results. Consequently, there is currently no consensus on which scaling methods would be best suited to achieve reliable median demand estimates over a wide range of structural properties, seismic hazard conditions, and hazard levels. Considering these issues, the research effort described in this paper is conducting a large number of small-scale shake-table experiments of re-configurable linear-elastic and nonlinear multi-story building frame structures using an exhaustive set of ground motion records. These shake-table tests will form the first experimental study on dynamic response considering a wide range of building properties, lateral strengths, and ground motion records. Ultimately, the results will not only provide the experimental evidence needed to evaluate different ground motion scaling methods, but will also investigate how different site parameters and structure characteristics affect the accuracy and efficiency of the scaling methods. After briefly discussing the current practices and challenges related to ground motion scaling, this paper summarizes the ongoing experimental research effort. Preliminary evaluation results for ground motion scaling are presented based on a linear-elastic test structure.

CURRENT PRACTICE AND CHALLENGES

Procedures for selecting and scaling ground motion records for a site-specific seismic hazard are broadly described in building codes and have been the subject of considerable research in recent years. The ground motion selection and scaling procedures in IBC (ICBO 2006) and CBC (ICBO 2007) are based on ASCE 7-05 (ASCE 2006). According to ASCE 7-05, the average 5%-damped linear-elastic acceleration response spectrum for a set of scaled records should not be less than the design spectrum over the period range from $0.2T_1$ to $1.5T_1$, where T_1 is the fundamental vibration period of the structure being designed. The design value of an engineering demand parameter (EDP) — member deformations, lateral drifts, floor accelerations, etc. — is taken as the average value of the EDP if seven or more records are used in the analysis, or its maximum value over all ground motions if the structure is analyzed for less than seven records (ASCE 7-05 requires a minimum of 3 records). These requirements for ground motion scaling are the same as those in the recently released ASCE 7-10 (ASCE 2010).

To demonstrate the challenges for the reliable use of nonlinear RHA in current practice, Figure 1 shows the estimated peak inter-story drift demands (Morgen and Kurama 2008) for a six-story reinforced concrete frame structure subjected to 10 pairs of “far-fault” MCE ground motion records satisfying the ASCE 7-05 scaling requirement. The drift demands from the 10 pairs of records range from a minimum of slightly less than 1% to a maximum of almost 5%. It is clear that if

only the peak demand from 3 records were used in design, as allowed by ASCE 7-05, then the design outcome (i.e., over-design, under-design, satisfactory) can be drastically altered depending on the records selected. Note that the demands in Figure 1 seem to be highly correlated with the ground motion maximum incremental velocity, MIV (Kurama and Farrow 2003), plotted on the x-axis.

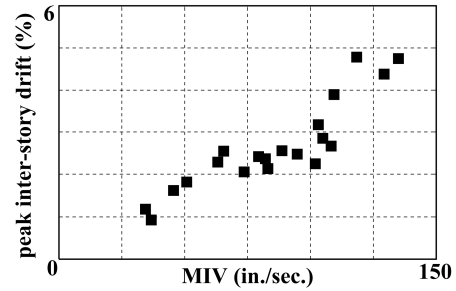


Figure 1. Peak drift demands.

GROUND MOTION SELECTION

Due to lack of specific guidelines, practitioners often select ground motion records based solely on distance, site conditions, and magnitude of the characteristic event expected to dominate the seismic hazard. However, many other factors, such as directivity of the rupture and/or basin effects contribute to the intensity and frequency content of a ground motion at a site. For example, as described in Kalkan and Kunnath (2006, 2008), “forward directivity” (with double-sided pulse) and “fling-step” (with single-sided pulse) motions with long-period, large-amplitude pulses may impose large displacement demands that require the structure to dissipate considerable energy in a single or relatively few cycles.

For the selection of the ground motions in this study, a set of criteria and identification algorithms were set to distinguish earthquake records based on their characteristic attributes associated with source, directivity, site, and/or basin effects (e.g., cyclic versus impulsive records; records with high, mid, or low frequency content; short or long duration records). Basin, duration, and pulse attributes of the records were investigated by frequency domain analyses; whereas, directivity and fling attributes were identified from the orientation of accelerometers relative to the rupture propagation plane. These attributes were then used to categorize a large library of records (PEER Next Generation Attenuation Project Ground Motions database) to facilitate the selection of the most suitable ground motions for different site-specific hazard conditions. Based on this refinement and pre-selection process, a suite of 38 representative near-fault motions (recorded within 20 km of the fault rupture) from a variety of tectonic environments were compiled for the purposes of this research as shown in Table 1.

EXPERIMENTAL STRUCTURE CONFIGURATION

The frame structure selected for the experimental investigation corresponds to a six-story building. As shown in Figure 2(a), the test frame consists of a single bay with center-to-center span length of 30 in. and story height of 17 in. These dimensions, determined based on the size limitations of the shake table, correspond to a building length-scale of, approximately, $S_L=1/10$. The chosen time scale is $S_T=1/3$. Two steel plates with total weight of 92.6 lb were securely attached to the midspan of each floor beam, and one plate with weight of 46.3 lb was attached to the midspan of the roof beam.

Table 1. Ground motion records.

EQ File ID	Earthquake Name	Station Name	Year	Magnitude
1058-E	Duzce, Turkey	Lamont 1058	1999	7.14
1059-N	Duzce, Turkey	Lamont 1059	1999	7.14
1061-E	Duzce, Turkey	Lamont 1061	1999	7.14
1062-E	Duzce, Turkey	Lamont 1062	1999	7.14
375-N	Duzce, Turkey	Lamont 375	1999	7.14
531-N	Duzce, Turkey	Lamont 531	1999	7.14
AMA090	Kobe, Japan	Amagasaki	1995	6.90
BOL090	Duzce, Turkey	Bolu	1999	7.14
BRN090	Loma Prieta	BRAN	1989	6.93
CAP000	Loma Prieta	Capitola	1989	6.93
CLS000	Loma Prieta	Corralitos	1989	6.93
CPM000	Cape Mendocino	Cape Mendocino	1992	7.01
DZC270	Duzce, Turkey	Duzce	1999	7.14
FKS090	Kobe, Japan	Fukushima	1995	6.90
FOR000	Cape Mendocino	Fortuna - Fortuna Blvd	1992	7.01
G02000	Loma Prieta	Gilroy Array #2	1989	6.93
G03000	Loma Prieta	Gilroy Array #3	1989	6.93
G04000	Loma Prieta	Gilroy Array #4	1989	6.93
G06090	Loma Prieta	Gilroy Array #6	1989	6.93
GIL067	Loma Prieta	Gilroy - Gavilan Coll.	1989	6.93
GOF160	Loma Prieta	Gilroy - Historic Bldg.	1989	6.93
HEC090	Hector Mine	Hector	1999	7.13
I-ELC180	Imperial Valley-02	El Centro Array #9	1940	6.95
KJM000	Kobe, Japan	KJMA	1995	6.9
LGP090	Loma Prieta	LGPC	1989	6.93
LOB000	Loma Prieta	UCSC Lick Observatory	1989	6.93
NIS090	Kobe, Japan	Nishi-Akashi	1995	6.90
PET090	Cape Mendocino	Petrolia	1992	7.01
PRI000	Kobe, Japan	Port Island (0 m)	1995	6.90
RIO360	Cape Mendocino	Rio Dell Overpass – FF	1992	7.01
SHI000	Kobe, Japan	Shin-Osaka	1995	6.90
SJTE225	Loma Prieta	San Jose - Santa Teresa Hills	1989	6.93
STG000	Loma Prieta	Saratoga - Aloha Ave	1989	6.93
TAK090	Kobe, Japan	Takatori	1995	6.90
TAZ090	Kobe, Japan	Takarazuka	1995	6.90
UC2090	Loma Prieta	UCSC	1989	6.93
WAH090	Loma Prieta	WAHO	1989	6.93
WVC270	Loma Prieta	Saratoga - W Valley Coll.	1989	6.93

The tests were conducted on a medium-size uniaxial earthquake simulator at the University of Notre Dame that consists of a hydraulic actuator/servo-valve assembly and a hydraulic power supply that drive a 4 ft by 4 ft slip table. Figure 2(b) depicts the test frame placed on the shake table, together with the measurement and out-of-plane bracing frames mounted onto the laboratory floor. The test frame was fabricated from extruded aluminum 6105-T5 alloy with a yield strength of 35 ksi. The beam and column member cross-sections were determined to result in strength and

stiffness appropriate with the scale model. The extruded aluminum cross-section in Figure 3(a), oriented in the weak direction (with moment of inertia, $I=0.7097 \text{ in.}^4$ and area, $A=3.00 \text{ in}^2$) was used for all beam and column members.

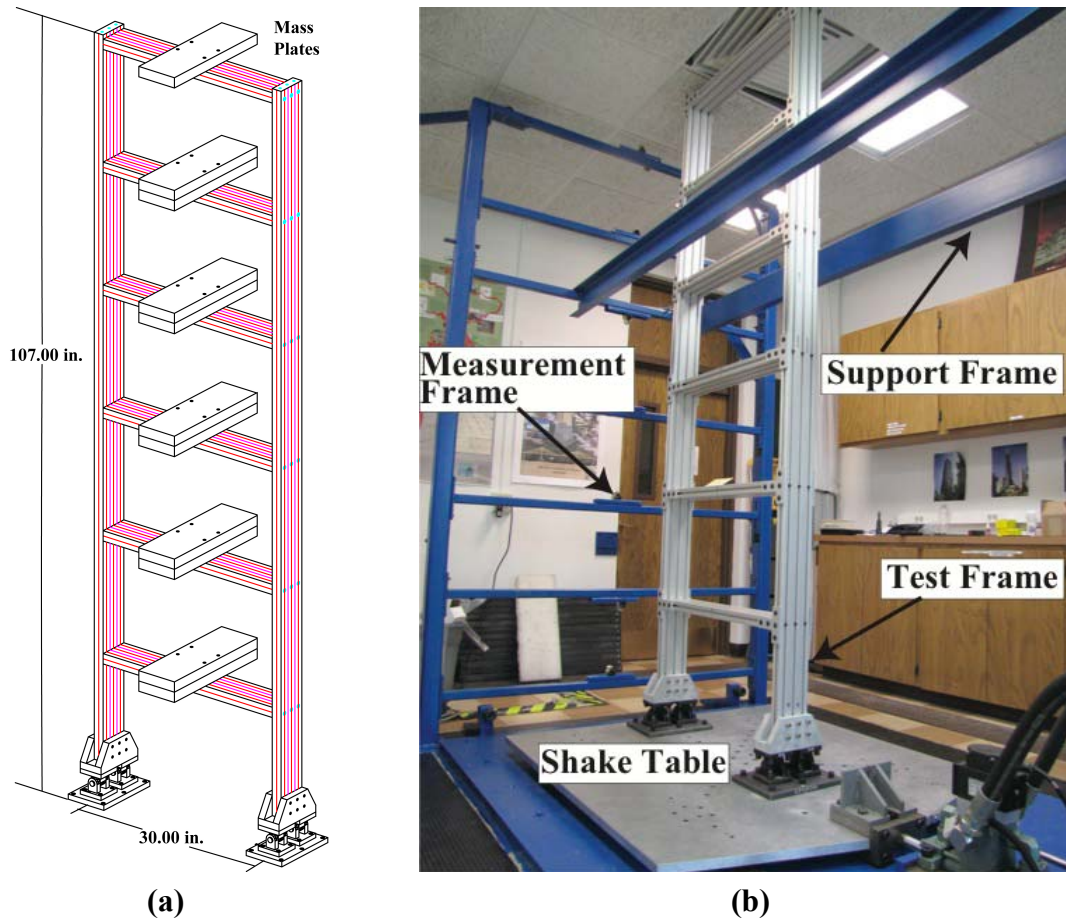


Figure 2. Six-story test frame: (a) schematic; (b) test setup.

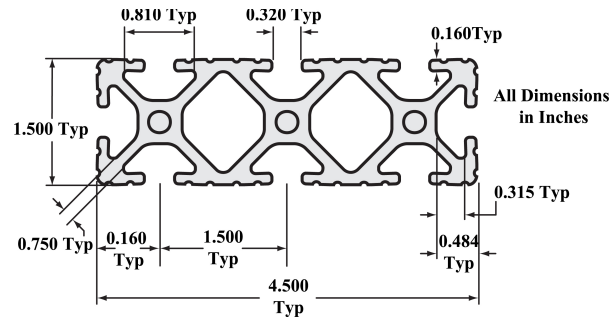
The shake table used in the experimental program can achieve a maximum acceleration of $\pm 4 \text{ g}$ with a 1000 lb test load at a nominal operational frequency range of 0-50 Hz. The data acquisition system is capable of recording the table displacements as well as the displacements and accelerations at each floor and roof level of the specimen. The data was collected at a high sampling rate, resulting in close-to-simultaneous excitation and response measurements. The displacements of the structure were measured using seven free unguided LVDTs (six at the floor and roof levels and one at the base) anchored between the test frame and an isolated measurement frame. An example of a mounted LVDT can be seen in Figure 3(b). The clamps used to attach the LVDTs to the measurement frame were engineered to mitigate vibrations.

The column bases were designed and constructed with pinned connections to increase the flexibility of the structure. Figure 3(c) depicts a close-up view of the pinned base connection. Each connection consists of a steel plate bolted to the shake table top, two steel clevises bolted to the plate, and two steel eye brackets inserted into the clevises and bolted to an aluminum fixture at the column base. A tight

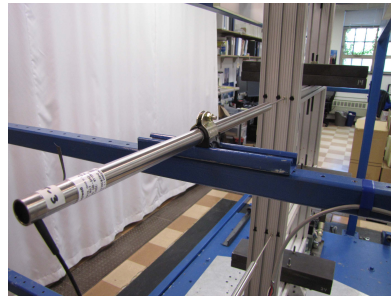
tolerance greased steel pin was used through the eye bracket-to-clevis connection to reduce friction while eliminating backlash effects. To achieve a modular structure, each beam-column connection was constructed using three high-strength bolts passing through the column and screwing into holes tapped into the beam cross section at each end.

A nonlinear beam-to-column connection is also being constructed as part of this project to allow for the future testing of nonlinear structures with different levels of lateral strength (corresponding to different response modification factors, R). As an important feature, the nonlinear connection will also be reconfigurable and reusable, so as to allow for the repeated testing of structures with different lateral strengths under a series of ground motion records. The design of the connection incorporates a friction-fuse concept previously investigated at the University of Notre Dame (Morgen and Kurama 2004). As shown in Figure 4, each beam-to-column connection consists of two components creating 10 rotational friction interfaces in between.

The nonlinear beam-to-column connection component bolted to the beam end will be fabricated out of stainless steel and the component bolted to the column will be lead-bronze (brass). The use of this alloy at the friction interfaces is desirable because the material continually “self-lubricates” when rubbing against an adjacent metal surface, which helps to reduce the phenomenon of stick-slip and results in a consistent value for the coefficient of friction that is relatively independent of velocity (a desirable characteristic for design and performance). The



(a)



(b)



(c)

Figure 3. Test details: (a) extrusion profile for beam and column members (courtesy 80/20[®] Inc.); (b) LVDT mounted to frame; (c) pinned connection at column base.

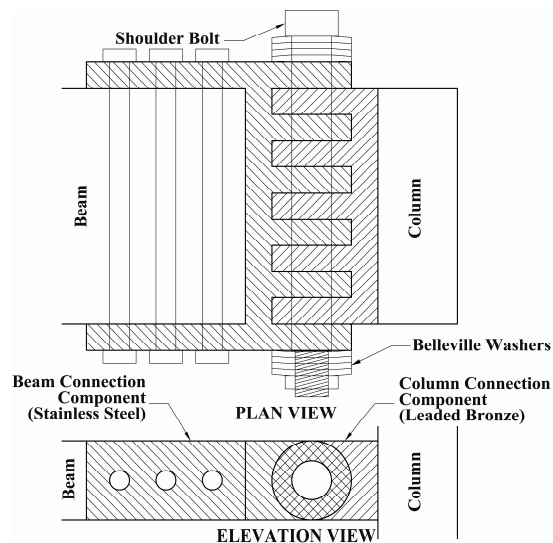


Figure 4. Nonlinear connection.

friction force can be controlled by the normal force, F_n applied on the interfaces. In the nonlinear beam-to-column connection, this will be achieved using a single high-strength shoulder bolt (see Figure 4) running through the 10 friction interfaces. The prototype connection was designed to produce a total maximum slip moment of about 35 kip-in. at the maximum normal force level. This slip moment was designed to be greater than the yield moment of the aluminum beam cross-section, and thus, it will be used to simulate a linear-elastic structure ($R=1$). As the normal force is decreased, the connection is allowed to slip at a smaller moment, simulating structures with lower lateral strengths (i.e., $R>1$) and nonlinear hysteretic response. Belleville washers will be used to maintain a consistent level of normal force across the friction interfaces during each test. After each test, the bolt through each connection will be loosened, the structure will be brought back to plumb, and the connection bolts will be re-tightened to the desired level. A combination of steel shims and Belleville washers will be used to consistently achieve the desired bolt force in each test. Prior to the use of the connections in multi-story frame testing, isolated beam-column subassemblies will be subjected to static and dynamic loads to characterize the nonlinear connection and calibrate the bolt tightening operation as well as the number/arrangement of the shims and Belleville washers to result in the target slip moment levels. This will ensure that the desired connection performance can be achieved with relative certainty and repeatability during the multi-story frame tests.

STATIC BEHAVIOR OF LINEAR-ELASTIC STRUCTURE

To investigate the stiffness characteristics of the linear test structure, monotonic and cyclic pushover experiments were conducted by holding the 4th floor of the frame stationary while displacing the base laterally using the shake table. At the 4th floor level, a steel rod with pin-ended connections (Figure 5) was placed between the test frame and a relatively stiff steel loading frame. As the base of the structure was displaced, the resulting 4th floor force in the pin-ended rod was measured using an intermediary load cell. Two string pot transducers were used to measure the absolute lateral displacements at the base and 4th floor level of the structure (note that the 4th floor displacements were very small but not zero due to the deformations of the loading frame).



Figure 5. Pin-ended rod and load cell assembly.

The 4th floor lateral force versus relative (with respect to base) 4th floor displacement results for the frame during two cycles of loading are shown using the thin black lines in Figure 6. The structure exhibited consistent and repeatable behavior in both the positive and negative loading directions; however, the onset of nonlinear behavior was observed at a relatively small load (about 500 lbs). It was found that the nonlinear behavior occurred as the beam ends lost full contact with the columns due to the stretching of the beam-column connection bolts. The flexibility of the connection bolts also reduced the initial lateral stiffness of the frame (i.e., the beam-to-column connections were not rigid as originally assumed).

Analytical models of the linear-elastic test structure were developed using the OpenSees and DRAIN-2DX programs. The flexibility of the beam-column connections (due to the flexibility of the connection bolts) was modeled by placing linear-elastic zero-length rotational springs at the beam ends. The stiffness of the rotational springs was determined by calibrating the model results (thick gray line) with the linear-elastic range of the measured behavior as shown in Figure 6.

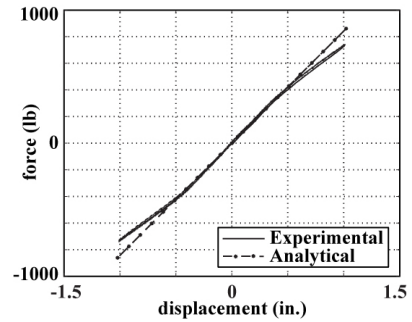


Figure 6. Measured and analytical static behaviors.

Once the nonlinear connection in Figure 4 is constructed and characterized, the hysteretic behavior of frames utilizing these connections will be determined. The analytical modeling of these frames will also utilize zero-length spring elements at the beam ends, but, unlike the linear-elastic frame, these spring elements will have nonlinear hysteretic behavior. The properties of the springs will be determined by calibrating the analytical results with the measured cyclic behavior of the frame, thus providing a full range of prediction tools.

DYNAMIC BEHAVIOR AND IDENTIFICATION

The dynamic characteristics of the linear-elastic structure were investigated by subjecting the frame to a series of sine sweep experiments. The results from three series of sine sweep tests with base excitation amplitudes ranging from 0.005 in. to 0.015 in. can be seen in Figure 7(a), where the y-axis shows the ratio of the relative roof displacement amplitude to the base excitation amplitude and the x-axis shows the frequency of the sine wave exciting the structure. While there is some amplitude dependency, it can be seen that the fundamental frequency of the structure is around $f_1=4.35$ Hz, (corresponding to a period of $T_1=0.23$ s), which was found to match very well with the analytical prediction. With the selected time scale of $S_T=1/3$, the test specimen corresponds to a full-scale structure with a fundamental period of about $T_1=0.69$ s. The second mode of vibration of the structure was measured to occur at around $f_2=16.1$ Hz, also with an excellent match with the analytical prediction. The measured mode shapes for the first two modes of vibration can be seen in Figure 7(b). Using the log decrement method on the decay of the measured displacement response at the roof, the damping ratio of the frame was determined as $\xi=1.14\%$. The time-history of the roof displacement used in this calculation can be seen in Figure 7(c).

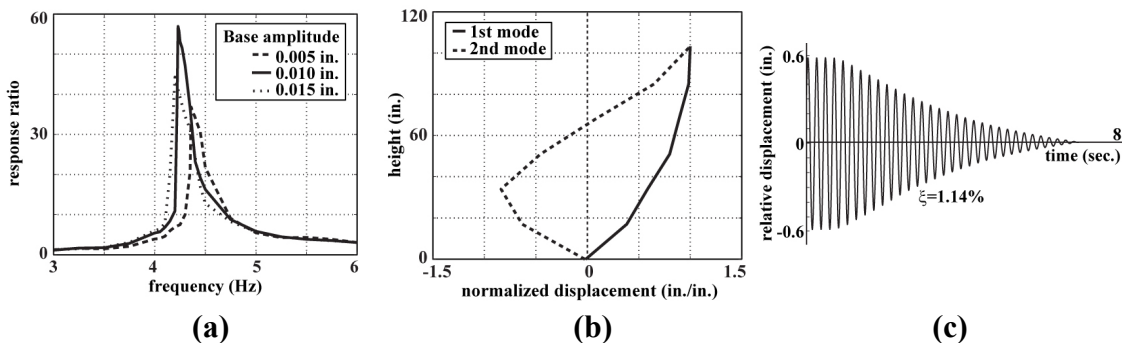


Figure 7. Dynamic behavior: (a) resonance peaks; (b) first and second mode shapes; (c) decay of roof displacement response.

A subset of earthquake ground motion records was selected and the measured dynamic response of the structure was compared with the estimated response from the OpenSees analytical model as another method of model calibration. Estimated versus measured roof displacement response comparisons from the AMA090 and CPM000 ground

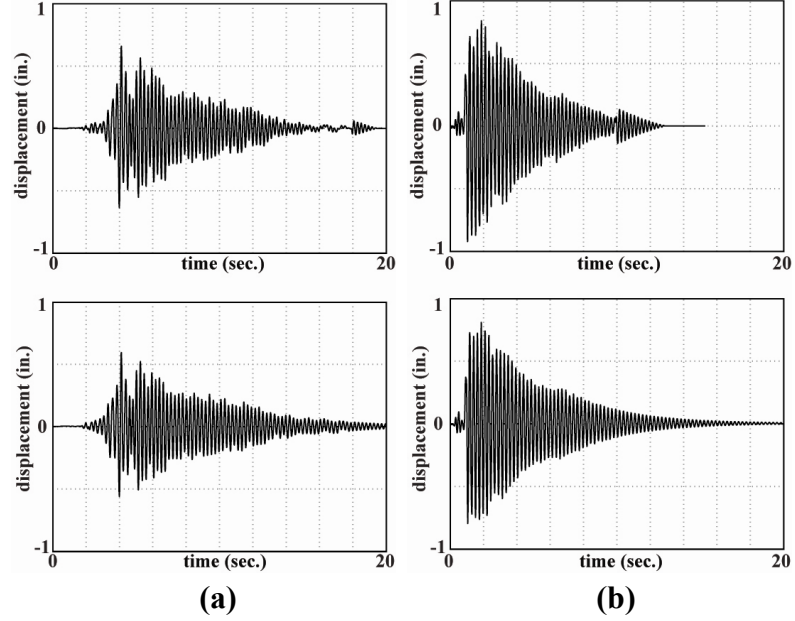


Figure 8. Measured (top) and estimated (bottom) roof displacement responses: (a) AMA090; (b) CPM000.

motion records can be seen in Figures 8(a) and Figure 8(b), respectively. Once the accuracy of the model was improved and deemed sufficient, the analytical model was subjected to the full suite of 38 ground motion records from Table 1 to guide the shake table tests described in the next section.

GROUND MOTION SCALING FOR LINEAR-ELASTIC RESPONSE

With the characteristics of the linear-elastic structure fully understood and the expected displacement demands from each ground motion estimated by the calibrated analytical model, the test specimen was subjected to five series of shake table tests using 37 ground motions from Table 1 (KJM000 was not used in the experiments due to excessive displacement demands indicated from the pre-test analysis of the structure under this record). The first series of tests subjected the specimen to the unscaled ground motions at full intensity. The second series was conducted with the ground motions scaled to the median linear-elastic single-degree-of-freedom spectral acceleration at the fundamental period of the structure $[\widehat{S}_a(T_1)]$. The effects of uncertainties in structural period estimation (i.e., inaccuracies in period estimation that could be expected in typical design practice) were investigated in the third and fourth test series. For this collection of tests, the ground motion suites were scaled to the median spectral acceleration at $1.3T_1$ and $0.7T_1$ [i.e., $\widehat{S}_a(1.3T_1)$ and $\widehat{S}_a(0.7T_1)$, respectively], representing a 30% error in period estimation. Finally, the fifth series of tests subjected the structure to ground motions scaled to the median maximum incremental velocity (\overline{MIV}) of the suite.

The peak roof displacement demands from the five series of experiments are plotted in Figure 9 and listed in Table 2. It can be seen that the unscaled peak displacement demands are not as strongly correlated to MIV as compared to the correlation with $S_a(T_1)$. As can be expected for a linear-elastic structure, the $\widehat{S}_a(T_1)$

scaling method produced the smallest dispersion in the peak roof displacements. However, the dispersion more than doubled with a 30% error in period estimation, with values similar to the dispersion from the MIV-scaled suite. These results are important in showing that inaccuracies in the estimation of a structure's anticipated period can lead to a much larger dispersion in the seismic demand estimates when compared with the dispersion achieved with the records scaled based on the "exact" period. The remainder of this project will investigate the effects of nonlinear structural response on these findings, including additional scaling methods in the investigation as well.

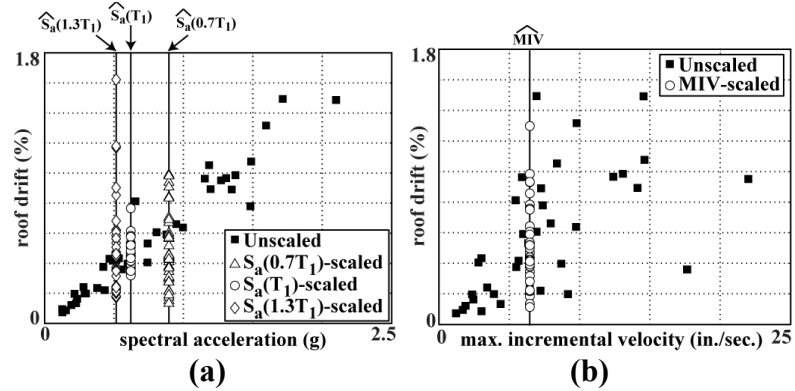


Figure 9. Peak roof displacement demands: (a) plotted against $S_a(T_1)$; (b) plotted against MIV.

SUMMARY AND CONCLUSIONS

This paper describes an ongoing research effort for a novel experimental evaluation of ground motion scaling methodologies for use in nonlinear response history analysis of building structures. The general experimental setup and the features of a 1/10-scale six-storey linear-elastic test frame structure are presented, along with identification results for the static and dynamic properties of the structure. Current efforts for extending the test structure to simulate nonlinear response, reconfigurable to different response modification factors, are also discussed. The test results from the linear-elastic structure stress the potential vulnerabilities of scaling methods that are based on knowledge of the exact properties of the structure. The future extension of this investigation to nonlinear dynamic response, considering a wide range of building properties, lateral strengths, and ground motion records, will ultimately provide guidelines and procedures for appropriate selection and scaling of ground motions for structural engineering practice.

ACKNOWLEDGEMENTS

This research is funded by the National Science Foundation (NSF) under Grant No. CMMI 0928662. The support of Dr. M.P Singh, NSF Program Director, is gratefully acknowledged. The authors would like to acknowledge the project advisory panel, which includes Paulo Bazzurro, AIR Worldwide Corporation, Sigmund Freeman, Wiss, Janney, Elstner Associates, Inc., Vladimir Graizer, U.S. Nuclear Regulatory Commission, Farzad Naeim, John A. Martin and Associates, Inc., and Thomas Sabol, Englekirk & Sabol Consulting Structural Engineers, Inc. The authors also thank Bob St. Henry of NEFF Engineering for his help in the design of the test

frame. The opinions, findings, and conclusions in the paper are those of the authors and do not necessarily reflect the views of the organizations or individuals above.

Table 2. Peak roof displacement responses for five series of linear-elastic tests.

GM Identifier	Unscaled	$\widehat{S}_a(T_1)$	$\widehat{S}_a(0.7T_1)$	$\widehat{S}_a(1.3T_1)$	\overline{MIV}
	in.	in.	in.	in.	in.
1058-E	0.09	0.40	0.43	0.44	0.19
1059-N	0.08	0.35	0.31	0.43	0.36
1061-E	0.10	0.55	0.44	0.39	0.42
1062-E	0.45	0.54	1.03	1.21	0.89
375-N	0.23	0.34	0.16	0.64	0.20
531-N	0.13	0.48	0.32	0.37	0.49
AMA090	0.66	0.38	0.36	0.18	0.39
BOL090	1.11	0.40	0.63	0.32	0.41
BRN090	1.09	0.64	0.46	0.88	0.81
CAP000	0.81	0.33	0.72	0.64	0.66
CLS000	1.36	0.39	0.61	1.22	0.78
CPM000	0.92	0.46	0.48	0.49	0.39
DZC270	1.02	0.43	0.98	0.36	0.45
FKS090	0.44	0.60	0.54	0.19	0.44
FOR000	0.14	0.48	0.45	0.21	0.19
G02000	0.61	0.41	0.59	0.93	0.63
G03000	0.55	0.46	0.32	0.60	0.54
G04000	0.24	0.39	0.19	0.24	0.22
G06090	0.17	0.43	0.40	0.45	0.41
GIL067	0.21	0.45	0.23	0.45	0.33
GOF160	0.21	0.39	0.23	0.26	0.14
HEC090	0.43	0.53	0.14	0.55	0.46
I-ELC180	0.84	0.79	0.87	0.48	0.96
LGP090	0.92	0.41	0.46	0.45	0.78
LOB000	0.25	0.53	0.29	0.42	0.44
NIS090	1.54	0.40	0.73	1.68	1.34
PET090	1.54	0.42	0.87	0.46	0.61
PRI000	0.37	0.40	0.39	0.23	0.12
RIO360	0.41	0.43	0.20	0.58	0.29
SHI000	1.00	0.53	1.02	0.70	1.02
SJTE225	0.42	0.36	0.70	0.63	0.96
STG000	0.63	0.48	0.72	0.58	0.55
TAK090	0.98	0.43	0.60	0.22	0.23
TAZ090	1.00	0.50	0.29	0.52	0.51
UC2090	0.20	0.60	0.47	0.46	0.54
WAH090	0.39	0.54	0.45	0.25	0.43
WVC270	0.68	0.45	0.94	0.48	0.53
MEDIAN	0.45	0.43	0.46	0.46	0.45
ST. DEV.	0.42	0.09	0.25	0.31	0.27

REFERENCES

- Alavi, B. and Krawinkler, H. "Consideration of near-fault ground motion effects in seismic design," *12th World Conference on Earthquake Engin.*, Paper No. 2665, Auckland, New Zealand, 2000.
- ASCE, "Minimum design loads for buildings and other structures," American Society of Civil Engineers, ASCE Standard No. ASCE/SEI 7-05, Reston, VA, 2006.
- ASCE, "Minimum design loads for buildings and other structures," American Society of Civil Engineers, ASCE Standard No. ASCE/SEI 7-10, Reston, VA, 2010.
- Chopra, A.K., and Chinatanapakdee, C., "Inelastic deformation ratios for design and evaluation of structures: single-degree-of-freedom bilinear systems," *J. of Structural Engineering*, 130(9), 2004, 1304-1319.
- International Conference of Building Officials (ICBO), International Building Code, Whittier, CA, 2006.
- International Conference of Building Officials (ICBO), California Building Code, Whittier, CA, 2007.
- Kalkan E. and Chopra A.K., "Practical guidelines to select and scale earthquake records for nonlinear response history analysis of structures," U.S. Geological Survey Open-File Report 2010-1068, 2010, 126 pp. (available online at <http://nsmmp.wr.usgs.gov/ekalkan/MPS/index.html>)
- Kalkan E. Chopra A.K., "Modal-pushover-based ground motion scaling procedure," *J. of Structural Engineering*, 137(3), 2011, (available online at <http://nsmmp.wr.usgs.gov/ekalkan/MPS/index.html>)
- Kalkan E. and Kunnath S.K., "Relevance of absolute and relative energy content in seismic evaluation of structures," *Advances in Struc. Eng.*, 11(1), 2008, 17-34.
- Kalkan E. and Kunnath S.K., "Effects of fling-step and forward directivity on the seismic response of buildings," *Earthquake Spectra*, 22(2), 2006, 367-390.
- Kalkan E. and Kwong N.S., "Documentation for assessment of modal pushover-based scaling procedure for nonlinear response history analysis of "ordinary standard" bridges," U.S. Geological Survey Open-File Report 2010-1328, 58 p. 2011, (available online at <http://pubs.usgs.gov/of/2010/1328/>).
- Kurama, Y. and Farrow, K., "Ground motion scaling methods for different site conditions and structure characteristics," *Earthquake Engineering & Structural Dynamics*, 32(15), 2003, 2425-2450.
- Martinez-Rueda, J., "Scaling procedure for natural accelerograms based on a system of spectrum intensity scales," *Earthquake Spectra*, 14, 1998, 135-152.
- Morgen, B. and Kurama, Y., "Seismic response evaluation of post-tensioned precast concrete frames with friction dampers," *J. of Str. Eng.*, 134(1), 2008, 132-145.
- Morgen, B. and Kurama, Y., "A friction damper for post-tensioned precast concrete beam-to-column joints," *PCI J.*, 49(4), 2004, 112-133.
- Shome, N. and Cornell, C., "Normalization and scaling accelerograms for nonlinear structural analysis," *6th U.S. National Conf. on Earthquake Engin.*, Seattle, WA, 1998 (CD-ROM).